BMC Biology

BioMed Central

Research article

Open Access

The functional organization of mitochondrial genomes in human cells

Francisco J Iborra[1], Hiroshi Kimura[2] and Peter R Cook*[3]

Address: [1]MRC Molecular Haematology Unit, Weatherall Institute of Molecular Medicine, John Radcliffe Hospital, Oxford, OX3 9DS, UK, [2]Nuclear Function and Dynamics Unit, HMRO, Graduate School of Medicine, Kyoto University, Kyoto 606-8501, Japan and [3]Sir William Dunn School of Pathology, University of Oxford, Oxford, OX1 3RE, UK

Email: Francisco J Iborra - francisco.iborra@imm.ox.ac.uk; Hiroshi Kimura - hkimura@hmro.med.kyoto-u.ac.jp; Peter R Cook* - peter.cook@path.ox.ac.uk

* Corresponding author

Published: 24 May 2004

BMC Biology 2004, **2**:9

Received: 11 December 2003
Accepted: 24 May 2004

This article is available from: http://www.biomedcentral.com/1741-7007/2/9

© 2004 Iborra et al; licensee BioMed Central Ltd. This is an Open Access article: verbatim copying and redistribution of this article are permitted in all media for any purpose, provided this notice is preserved along with the article's original URL.

Abstract

Background: We analyzed the organization and function of mitochondrial DNA in a stable human cell line (ECV304, which is also known as T-24) containing mitochondria tagged with the yellow fluorescent protein.

Results: Mitochondrial DNA is organized in ~475 discrete foci containing 6–10 genomes. These foci (nucleoids) are tethered directly or indirectly through mitochondrial membranes to kinesin, marked by KIF5B, and microtubules in the surrounding cytoplasm. In living cells, foci have an apparent diffusion constant of 1.1×10^{-3} $\mu m^2/s$, and mitochondria always split next to a focus to distribute all DNA to one daughter. The kinetics of replication and transcription (monitored by immunolabelling after incorporating bromodeoxyuridine or bromouridine) reveal that each genome replicates independently of others in a focus, and that newly-made RNA remains in a focus (residence half-time ~43 min) long after it has been made. This mitochondrial RNA colocalizes with components of the cytoplasmic machinery that makes and imports nuclear-encoded proteins – that is, a ribosomal protein (S6), a nascent peptide associated protein (NAC), and the translocase in the outer membrane (Tom22).

Conclusions: The results suggest that clusters of mitochondrial genomes organize the translation machineries on both sides of the mitochondrial membranes. Then, proteins encoded by the nuclear genome and destined for the mitochondria will be made close to mitochondrial-encoded proteins so that they can be assembled efficiently into mitochondrial complexes.

Background

Mitochondria are the centre of energy production in the cell. They are usually numerous and polymorphic, and their overall shape depends on a balance between the fusion and fission of individual mitochondria [1]. These processes are controlled by several proteins [2], including dynamin-related protein 1 (Drp1) [3,4], and the mitofusins (for example, Mfn 1 and 2) [5]. Mitochondria also move in a complex way through living cells [6], probably carried by actin/myosin- and dynein/kinesin-based motors along the microfilament and microtubule networks [7,8].

In most human cells, mitochondria contain 10^3–10^4 copies of a circular genome of 16,569 base-pairs that encodes two ribosomal RNAs, 22 tRNAs, and 13 polypeptides that

form parts of the respiratory-chain located in the inner mitochondrial membrane [9,10]. A noncoding regulatory region harbours an origin of replication plus two promoters, one on each of the two strands. Transcription from these promoters generates polycistronic transcripts that are processed to produce mature rRNAs, tRNAs, and mRNAs; a transcript generated from one of the promoters also primes mitochondrial DNA (mtDNA) replication. Protein-coding regions of the resulting RNAs are translated by ribosomes within the mitochondrion. However, most mitochondrial proteins are encoded by the nucleus; they are made by cytoplasmic ribosomes and imported through specialized pores into mitochondria where they combine with those encoded by the mitochondrial genome [11,12].

As might be expected, mutations affecting mitochondria lead to a complex set of pathologies and the resulting disorders are the most frequent of the inborn errors of metabolism, with an estimated incidence of at least one in 10,000 live births [13]. Some causative mutations arise in the nuclear genome (for example, in *NDUFS4*, *7*, and *8* in Leigh and Leigh-like syndromes), others in the mitochondrial one. For example, A to G transitions in nucleotides 3243 and 8344 in mtDNA underlie mitochondrial encephalopathy with lactic acidosis and stroke-like episodes (MELAS) and myoclonic epilepsy with ragged red fibres (MERFF), respectively. Unlike normal individuals in whom most mtDNA copies are genotypically similar (homoplasmic), most patients suffering from mtDNA disorders have dissimilar copies (heteroplasmic). Therefore, it is of interest how the number of copies of mtDNA is regulated, how homoplasmy is maintained in normal individuals, and how quickly mutations spread through the mtDNA population to give rise to the mutant phenotype [13-15]. Unfortunately, we still lack precise answers to such questions in man as not enough is known about the organization of individual genomes; fortunately, more is known about the organization in yeast [1,2].

We now examine the organization of mitochondrial genomes in a human cell line that contains mitochondria tagged with the yellow fluorescent protein (YFP). This line is derived from the bladder carcinoma line, ECV304 – which is also known as T-24 [16] – and individual mitochondria can easily be seen in the thin cytoplasm of these epithelial-like cells.

Results

A stable cell line with YFP-tagged mitochondria

We first derived a stable cell line containing mitochondria tagged with the yellow fluorescent protein (YFP). A plasmid encoding subunit VIII of cytochrome c oxidase fused with YFP was transfected into an epithelial-like human line derived from a bladder carcinoma (ECV304), and a clone (cox18) expressing YFP was established. Expression of the plasmid in other cells has no effect on viability [17]. The tagged subunit is incorporated into mitochondria, making them autofluorescent (Figure 1A). However, photobleaching experiments show it diffuses rapidly throughout the interior of the mitochondrion ([17]; our unpublished results); this makes it unlikely that it is incorporated into the membrane to become functional. This clone is used for all experiments described here.

mtDNA is concentrated in foci in fixed cells

Mitochondrial DNA was localized in fixed cells in two ways. In one, it was immunolabelled using an anti-DNA antibody (Figure 1B); in the other, cells were grown for one generation in bromodeoxyuridine (BrdU) to label their DNA uniformly before the resulting Br-DNA was detected using an anti-Br antibody (Figure 1D). In both, mtDNA was found in roughly the same number of foci scattered along the length of mitochondria (Figure 1A,1B,1C,1D; Table 1) [18,19]. The mtDNA foci were more uniformly spaced than expected of a random distribution (Figure 1E); for example, 86% lay <1.2 μm apart, compared to the ~67% expected of a random distribution (significance >99.999% using Student's t test). This distribution probably arises as foci are not free to diffuse (below). The foci also had a range of intensities (Figure 1F).

Superficial examination of images like those in Figure 1A,1B,1C,1D also suggests that foci were concentrated in regions poor in the YFP-tagged subunit of cytochrome oxidase, which is distributed throughout the mitochondrial matrix (above). This was confirmed using a cross-correlation analysis. Twelve image pairs like those in Figure 1A and 1B were pseudo-coloured green and red respectively, the red component shifted over various distances (Δx) with respect to the green component, and the value of Pearson's correlation coefficient (r_P) plotted against Δx. If the red and green patterns coincide, mutually exclude each other, or are arranged randomly, r_P respectively peaks, dips, or remains flat, around a Δx of zero [20]. YFP proves to be excluded for up to 400 nm from the centre of mtDNA foci (Figure 1G), perhaps because mitochondria are thinner in this region [21]. This might be advantageous to the cell, as there would be less functional cytochrome oxidase in the thinner region to generate damaging free radicals near the mtDNA.

Immunogold labelling and electron microscopy confirmed that mtDNA was found in discrete sites; moreover, the sites often abutted the inner mitochondrial membrane as in Figure 2A. DNA also remained associated with cytoskeletal elements when mitochondrial membranes and most cytoplasmic proteins were extracted (Figure 2B), consistent with earlier results [22-24]. These sites had an

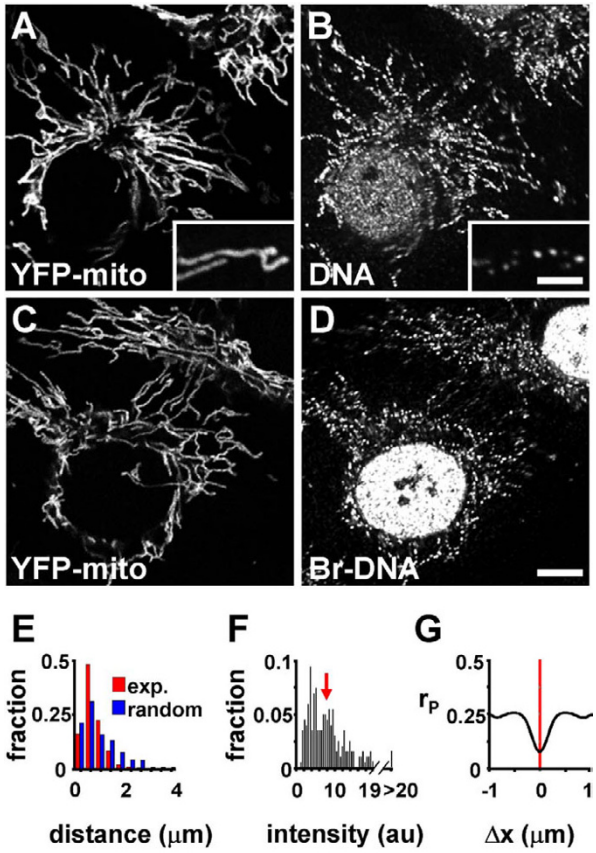

Figure 1
DNA in the mitochondria of fixed ECV-304 cells expressing subunit VIII of cytochrome oxidase tagged with YFP. **(A,B)** Two views taken with a confocal microscope of fixed cells after immunolabelling DNA. Mitochondria marked with YFP (A) contain discrete foci of mtDNA (B); nuclear DNA appears weakly labelled, presumably because most of it is inaccessible to the anti-DNA antibody, an IgM. Pretreatment (60 min; 20°C) with 25 μg/ml DNase removed >96% foci like those in (B). Insets: high-power views (bar: 2 μm). **(C,D)** Two similar views after growth (24 h) in BrdU, and immunolabelling the resulting Br-DNA; Br-DNA is found in nuclei and mitochondrial foci. Bar: 4 μm. **(E)** The distribution seen experimentally (exp) of distances between consecutive DNA foci within mitochondria (determined using images like (B); n > 500) differs significantly from a random one (p = 0.0013); foci tend to be closer together than expected. Distances (μm) are binned (that is, 0–0.4, 0.4–0.8, etc). **(F)** Experimental distribution (determined using 15 images like (D)) of intensities of mtDNA foci. Intensities (arbitrary units, au) are binned (that is, 0–0.5, 0.5–1, etc), the first bin contained no examples, and the arrow marks the average intensity. If the weakest focus (in bin 2) contains one genome, then the average contains ~9.2. **(G)** Cross-correlation analysis of mtDNA foci and the YFP-tagged subunit (using images like those in the insets in (A,B)); the low Pearson's coefficient (r_P) at Δx values close to zero indicates that mtDNA is excluded from sites containing YFP.

average diameter of ~68 nm (Table 1, line 4). As expected [2,7,25], mitochondria also associated with microtubules (Figure 3A,3B,3C,3D). Moreover, the kinesin motor implicated in moving mitochondria along microtubules – KIF5B [25] – often colocalized with individual mtDNA foci (Figure 3E,3F,3G), and a close association was confirmed by the peak in Pearson's coefficient at a Δx of zero (Figure 3H). These results are consistent with mtDNA foci being tethered through mitochondrial membranes to kinesin and the microtubule network.

A mtDNA focus contains approximately eight genomes

The number of mitochondrial genomes per focus was calculated after measuring the number of mitochondrial genomes per cell, the total mitochondrial length, and the number of foci per unit length of mitochondria (Table 1). While the first two can be estimated reasonably accurately, it is difficult to be sure that all foci are detected. Therefore we used various approaches, reasoning that if different methods with different thresholds of detection gave similar results, one estimate would lend credibility to another (Table 1, line 6). The data were analyzed as follows: (i) immunolabelling with both anti-DNA and anti-BrdU (after growth in BrdU to substitute DNA fully) gave similar results (that is, ~7 genomes/focus); (ii) the average intensity of foci in images like that in Figure 1D had an intensity 9.2× higher than the weakest (Figure 1F, legend); if the faintest focus then contains one genome, the average would contain ~9; (iii) foci had a diameter of ~68 nm (Table 1, line 4), sufficient to accommodate ~6 genomes packed as tightly as in the bacterial nucleoid [26]; and (iv) analysis of replication rates are consistent with each focus containing ~10 genomes (below). Taken together, these results suggest the average focus contains 6–10 genomes, again consistent with earlier results [18,19].

Dynamics of mtDNA in living cells

The dynamics of mtDNA in living cells can be monitored after staining with fluorescent dyes like 4',6'-diamidino-2-phenylindole (DAPI) [27], SYTO13 [28], or ethidium [29]; here, we use ethidium. Cells were grown briefly in 0.1 μg/ml ethidium, washed, and regrown in its absence; some dye is then seen in nuclei and mitochondria, with little in the rest of the cytoplasm. (This brief exposure has no long-term effects on cell doubling, but transcription is temporarily inhibited as bromouridine (BrU) incorporation into mitochondrial RNA falls to 60% of controls (measured as in Figure 7H (see later) during the 20 min following removal of ethidium; 1 μg/ml ethidium completely inhibits incorporation; not shown).) Immediately after exposure to 0.1 μg/ml, ethidium fluorescence in mitochondria is concentrated in discrete foci against a diffuse background (Figure 4B). On regrowth in the absence of ethidium, foci faded much less rapidly than the background; as a result, foci could still be seen after 8 h against

Table 1: Properties of mitochondria and their genomes.

Property	Value
Mitochondria	
1. total length/cell (μm)	600 ± 124[a]
mt DNA foci	
2. lineal density in mitochondria (foci/μm)	0.78[b], 0.82[c]
3. foci/cell	468 ± 97[d], 492 ± 102[e]
4. diameter (*range*; nm)	70[f], 65 (*31–132*)[g]
mtDNA	
5. molecules/cell	3,500[h]
6. molecules/focus	7.5[i], 7.1[j], 9.2[k], 5.8[l], 10[m]

[a]using stacks of images of 50 cells (one image from a stack is shown in Figure 1A). [b]using anti-DNA as in Figure 1A,1B; 43 cells analyzed. [c]using anti-BrdU as in Figure 1C,1D; 38 cells analyzed. [d]from rows 1 and 2 (anti-DNA). [e]from rows 1 and 2 (anti-BrdU). [f]from 120 clusters of gold particles like that in Figure 2A, after correcting for sectioning effects). [g]from 97 clusters of gold particles like that in Figure 2B. [h]from gel electrophoresis; value similar to that found by Jacobs *et al*. [14]. [i]from rows 3 (anti-DNA) and 5. [j]from rows 3 (anti-BrdU) and 5. [k]from mean intensity in Figure 1F, assuming the faintest focus contains 1 molecule. [l]from row 4 (unextracted cells), assuming DNA of 16.5 kbp is packed at 35 mg/ml (that is, the density of the bacterial nucleoid) [26] into a sphere (diameter 68 nm). [m]from replication pattern (Figure 6).

a now non-fluorescent background. This suggests that foci reflected tight binding to mtDNA, and the initial background an unstable binding to RNA. Marking RNA in fixed cells using a tagged RNA-binding protein (that is, RNase tagged with Cy3) confirms that this background contains RNA (see Methods).

After washing away ethidium, the fluorescent mtDNA foci can be seen moving continually within the (moving) mitochondria. This is illustrated using frames from time-lapse movies in which images were collected every 10 s for up to 500 s (Figure 4A,4B,4C,4D). Thus, the distance separating two adjacent foci labelled S1 in Figure 4B remained roughly constant at ~3 μm, although one focus travelled ~14 μm over 500 s. Similarly, the distance separating a terminal focus from the adjacent mitochondrial tip (S2 in Figure 4B) was always <1 μm, even though the tip moved 21 μm.

Movement of foci is superimposed on that of mitochondria, and it was analyzed in various ways [30]. The mean square displacement (MSD) of one mtDNA focus relative to another is >0 (Figure 4F, 'DNA'), but less than that of a tip of one mitochondrion relative to another (Figure 4F, 'tip'). An apparent diffusion constant (*D*) for mtDNA foci of 1.1×10^{-3} μm²/s was calculated from the MSD; this is comparable to that of DNA in *Drosophila* nuclei [30]. We next searched for directed or periodic movement using an autocorrelation function (ac) that relates changes in distance (Δd) seen between foci at increasing time intervals (Δt) [31]. The correlogram in Figure 4G is consistent with a random walk (step length 0.26 μm over 10 s) in which the direction changes every ~16 s, and with only ~4% steps continuing in the same direction for ≥40 s. The distribution of Δd was normal and centred on zero (Figure 4H), also indicative of a random walk [30].

Fission and fusion of mitochondria next to mtDNA foci

In 25 films of 20 min duration, ~6% mtDNA foci were seen to split (Figure 5A). If fission were coupled to replication, and as mtDNA is replicated throughout the cell cycle [32], we would expect only ~1.5% foci to split (since these cells have a cycle of ~22 h or ~1,320 min, and 20/1320 × 100 = 1.5); therefore, fissions seem uncoupled to replication. While some foci split, others fuse (Figure 5B); some fuse and remain together for 30–600 sec before splitting (not shown). In 49 out of 50 fusion-fission events the emerging foci retained the intensities of fusing foci.

Whole mitochondria also split, which in ~90% cases occurred by progressive thinning next to a focus to leave all DNA in one daughter (Figure 5C) [33]. As a result, some daughters arise that lack mtDNA, albeit rarely (not shown). That fission occurs next to mtDNA was confirmed by counting the fraction of mitochondrial tips in fixed cells that contained mtDNA within 500 nm of a tip (Figure 1A,1B, insets); the value (that is, 52%) was significantly higher than the 39% expected if mtDNA were distributed randomly along mitochondria ($p < 0.0001$; χ^2 test). As the dynamin-related protein, Drp1, is found at fission sites [34], we immunolocalized it relative to mtDNA, and found it often lay immediately next to mtDNA (Figure 5D,5E). This was confirmed by the peaks flanking the dip in Pearson's coefficient (r_p) around a Δx of zero (Figure 5F). These results confirm and extend those of Garrido *et al*. [35], and show that mitochondria split next to mtDNA foci.

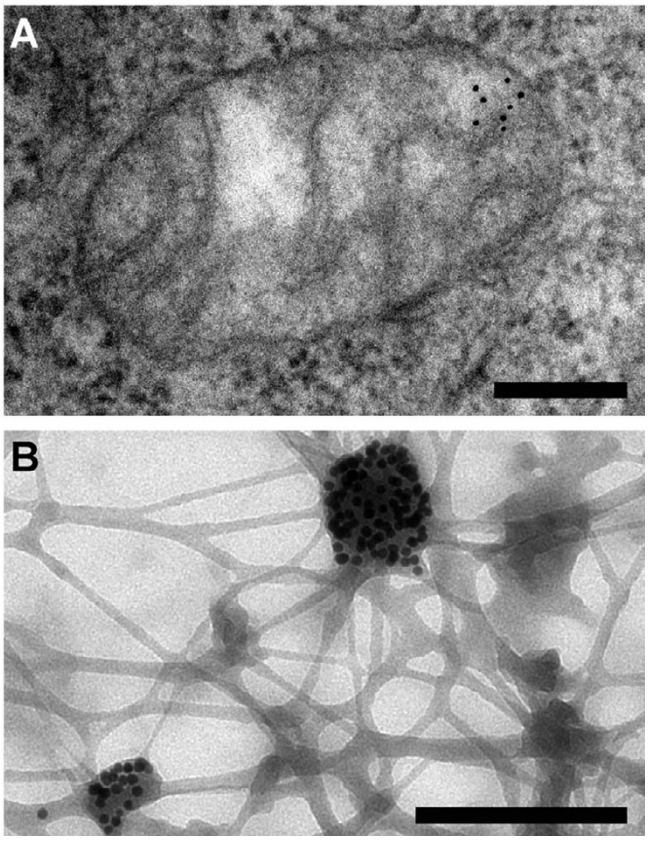

Figure 2
Electron microscopy reveals mitochondrial DNA in discrete foci. Bars: 200 nm. **(A)** Cytoplasmic section after immunogold labelling with anti-DNA; gold particles marking mtDNA are found near the mitochondrial membrane. **(B)** Whole mount view of cytoplasm after extraction with CSK buffer and immunogold labelling with anti-DNA; mtDNA (marked by gold particles) resists extraction.

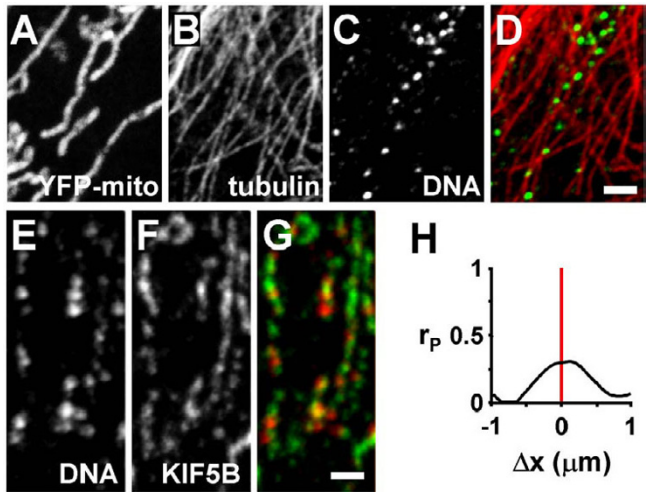

Figure 3
mtDNA associates with tubulin and a kinesin subunit (KIF5B). Cells with YFP-tagged mitochondria were fixed, various targets immunolabelled and imaged in the confocal microscope. **(A-D)** Four views of one region of the cytoplasm; mtDNA foci are found in mitochondria that are generally aligned with microtubules (mtDNA and tubulin are pseudocoloured green and red in the merge in (D)). Bar: 2 μm. **(E-G)** Three views of one region of the cytoplasm; mtDNA foci often lie near KIF5B (pseudocoloured red and green in the merge in (G)). Bar: 1 μm. **(H)** The high Pearson's coefficient (r_p) at Δx values close to zero indicates that mtDNA lies near KIF5B.

Stochastic replication of individual mitochondrial genomes

In mouse L cells, individual mtDNA molecules are selected randomly for replication throughout the cell cycle [32]. Active sites of synthesis can be localized after growing cells in BrdU, and then immunolabelling the resulting Br-DNA; Davis and Clayton [36] found that perinuclear mitochondria appear to be more synthetically active than peripheral ones. However, when we repeated this experiment, we found mitochondria in different regions were equally active, although the perinuclear region contained a higher concentration of mitochondria (Figure 6A,6B,6C). A similar result to ours has been obtained recently by Magnusson *et al.* [37]. The differences seen could arise from intrinsic differences between the cell types studied, or from an improved detection of Br-DNA at the periphery (where there are fewer mitochondria). The number of labelled foci increased on growth in BrdU for 3 h and then remained constant (Figure 6C); conversely, the average intensity per focus initially remained constant for 2 h and then increased (Figure 6D).

Three extreme models for the labelling kinetics are shown in Figure 6E; only one (model b) is consistent with essentially all foci containing some Br-DNA by 3 h (Figure 6C), and with the average intensity per focus being constant between 1 and 2 h before rising (Figure 6D). Then, one genome per focus would be replicated within the first 2 h, and all genomes in a focus after a complete cycle of 22 h. As the intensity per focus increases 10-fold during this period, we estimate each focus contains ~10 genomes (Table 1, line 6).

Newly-made mitochondrial transcripts are found in discrete sites

Sites containing newly-made RNA can be visualized after growing cells in bromouridine (BrU), and then immunolabelling the resulting Br-RNA [38,39]. (Here, cells are grown in the absence of ethidium so transcription is not

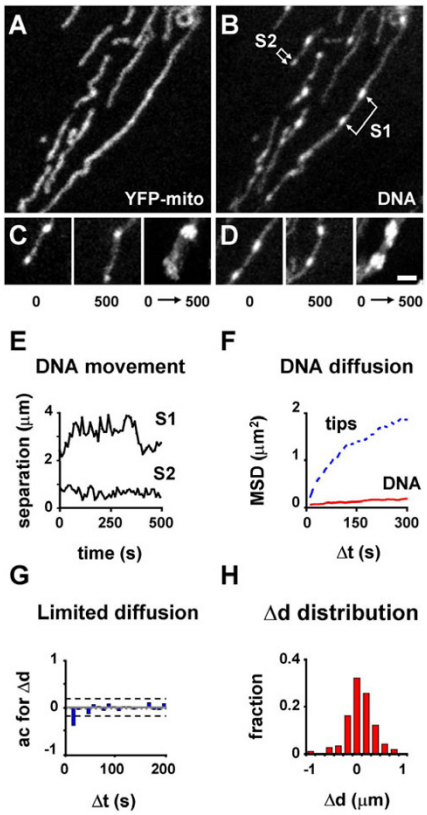

Figure 4
mtDNA dynamics in living cells with YFP-tagged mitochondria. Cells were grown (30 min) in 0.1 μg/ml ethidium, the ethidium washed away, the cells regrown for 10 min, and single confocal sections collected every 10 sec for ≤500 sec; mitochondria and mtDNA are marked by YFP and ethidium respectively. **(A,B)** Two views of mitochondria in one cell at one time. Ethidium is locally concentrated in (mtDNA) foci, against a background (bound to RNA). S1: distance between two foci. S2: distance between one focus and mitochondrial tip. **(C,D)** Frames showing ethidium fluorescence (marking mtDNA) from two movies. In each case, the first (0 sec; left) and last (500 sec; middle) frames show the two mtDNA foci move little relative to each other; this is confirmed by superimposing all frames in each movie (right). Bar: 2 μm. **(E)** Changes in separations S1 and S2 seen in (B) over time; movement is erratic. **(F)** Mean square displacement (MSD; n = 20) of one mt DNA focus relative to another (DNA), or one tip relative to another (tip); movement of foci is more restrained than that of tips. The MSD of one terminal focus relative to the tip is similar to that of one focus relative to another and is not shown. **(G)** Autocorrelation analysis. The autocorrelation (ac) between the displacement distances (Δd) for time points separated by different time intervals (Δt) of 10 sec (dashed lines show limits of 5% significance). The pattern is typical of a random walk; there is no periodicity, and the first value (the only significant one) is negative. (H) The distribution of step lengths (Δd) is typical of a random walk. Mean = 0.01 μm (SD ± 0.4). The maximum value was 2.4 μm, and is not shown.

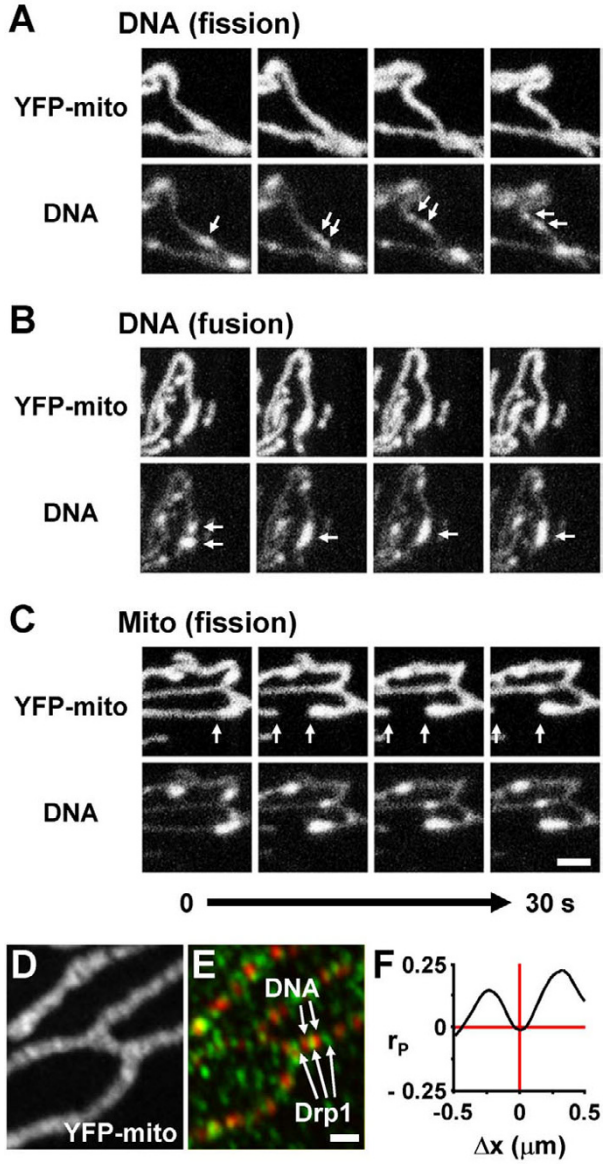

Figure 5
Fusion and fission of mitochondria and mtDNA foci. **(A-C)** Four pairs of frames (collected at 10 s intervals) from three movies of living cells (made as in Figure 4A,4B) showing YFP and ethidium fluorescence (marking mitochondria and mtDNA, respectively) are illustrated. Arrows mark a mtDNA focus that splits (A), two foci that fuse (B), and the point where a mitochondrion splits next to one mtDNA focus to give two separate tips (C). Bar: 1 μm. **(D-F)** Cells with YFP-tagged mitochondria were fixed, DNA and Drp1 immunolabelled with Cy5 and Cy3, and imaged; two views of one cell are shown in (D) and (E). In the merge (E), mtDNA often lies next to Drp1, which is also found in the cytoplasm [34]. Bar: 1 μm. A cross-correlation analysis of the distribution of mtDNA and Drp1 (data from 15 images like those in (D,E)); Pearson's coefficient (r_P) indicates that Drp1 is excluded from ~0.3 μm to each side of mtDNA foci (F).

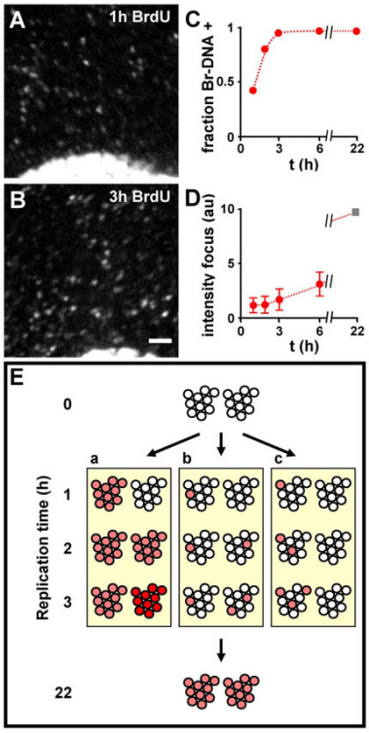

Figure 6
Mitochondrial replication. Cells with YFP-tagged mitochondria were grown in BrdU for 1–6 h, fixed, and Br-DNA immunolabelled. **(A,B)** On growth in BrdU, progressively more mitochondrial foci containing Br-DNA are seen. Bar: 2 μm. **(C)** Changes in the fraction of DNA foci containing Br-DNA (assuming cells contain 468 foci/cell; Table 1, line 3); essentially all foci contain Br-DNA within 3 h. **(D)** Integrated intensity of Br-DNA labelling per focus (in arbitrary units, with the value at 1 h set to unity). The average intensity per focus is constant between 1 and 2 h, and then rises; extrapolating the line from 2–6 h to 22 h (the length of the cell cycle) gives an intensity of 10 (square). **(E)** Three models for replication. Two DNA foci, each initially containing 10 unreplicated genomes (open circles), are shown. (a) Here, a focus is a unit of replication. In the first hour, all genomes in one focus replicate together (red circles) and half the foci become labelled (as in Figure 6C); in the second hour, all genomes in a second focus replicate together so that all genomes are now labelled (again as in Figure 6C). However, during the third hour, the intensity of foci continues to increase (Figure 6D), so we would have to assume that genomes re-replicate (dark red circles) and some would presumably have to be degraded to maintain genome numbers. (b) All genomes replicate independently of all others. The kinetics in (D) and (E) are consistent with this model. (c) Here, a polymerizing complex transfers from genome to genome in one focus before going to another focus; then genomes in one focus would replicate successively, before replication switched to another focus. This would give the progressive increase seen in Figure 6D, but many foci would remain unlabelled after 2 h (which is inconsistent with Figure 6E).

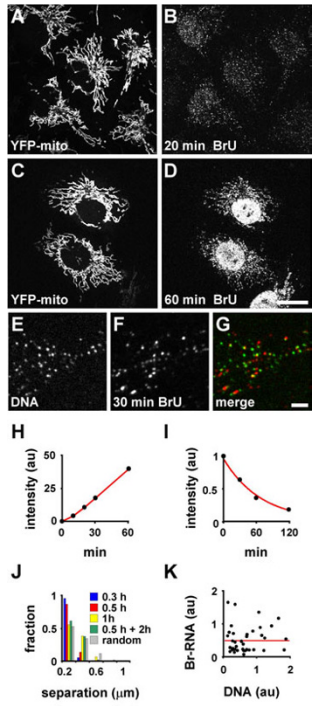

Figure 7
Mitochondrial transcription. Cells with YFP-tagged mitochondria were grown in 2.5 mM BrU for different times, fixed, Br-RNA immunolabelled with Cy3, and confocal images collected. In some cases, cells were grown for 30 min, washed, and regrown in 5 mM U for up to 2 h (I,J); in others, DNA was immunolabelled with Cy5 (E-G,J) or stained with Hoechst 33342 (K). **(A,B)** Two views of one field; after growth in BrU for 20 min, Br-RNA is seen mainly in mitochondria. **(C,D)** Two views of one field; after growth in BrU for 60 min, Br-RNA is seen mainly in nuclei. Bar: 10 μm. **(E-G)** Three views of mitochondria of one cell, after growth in BrU for 30 min and immunolabelling DNA with Cy5; the merge reveals Br-RNA (red) in some, but not all, mtDNA foci (green). Bar: 2 μm. **(H)** On growth in BrU, the intensity of Br-RNA labelling (arbitrary units/μm^2) in mitochondria increases progressively. **(I)** After growth for 30 min in BrU and regrowth in U, the intensity of mitochondrial Br-RNA labelling falls exponentially (red line; $t_{1/2} \sim 45$ min). **(J)** The effects of incubation time on distance between a Br-RNA focus and the nearest mtDNA focus. Distances (μm) are binned (that is, 0–0.2, 0.2–0.4, etc). After 20 or 30 min in BrU, most Br-RNA foci lie between 0–0.2 μm of the nearest mtDNA foci (labelled with Cy5); however, after 1 h (or a 30 min pulse followed by a 2 h chase), Br-RNA foci appear to be spread randomly. The decline in Br-RNA colocalizing with mtDNA (that is, lying within 0.2 μm) between 20 and 60 min is consistent with a residence half-life of 43 min. **(K)** After growth in BrU for 30 min, the intensity of labelling in a Br-RNA focus (au, arbitrary units) does not correlate with the DNA concentration seen in the associated mtDNA focus. The line (slope = 0.0042) is that of best fit. In an analogous experiment in which mtDNA was marked with the antibody, the line of best fit had a similar slope of 0.0068.

inhibited.) Br-RNA accumulates in nuclei and in discrete mitochondrial foci (Figure 7A,7B,7C,7D) that initially lie immediately next to mtDNA foci (Figure 7E,7F,7G). The intensity of Br-RNA labelling per focus increases progressively (Figure 7H), and declines exponentially ($t_{1/2} \sim 45$ min) during a 'chase' (Figure 7I). Quantitative analysis shows that after an initial pulse of 20 or 30 min, most Br-RNA foci colocalize with mtDNA (defined as lying within 200 nm of mtDNA), but after longer periods (or a pulse-chase) the Br-RNA foci become distributed randomly (Figure 7J). Kinetics are consistent with Br-RNA having a residence half-life in mtDNA foci of ~43 min (see Methods). This is approximately eight-fold longer than the ~5.5 min required to make a complete transcript (assuming ~50 nucleotides are polymerized every second) [40]. This suggests that mitochondrial messages remain at transcription sites for extended periods after they have been made.

Not all mtDNA foci contain Br-RNA (Figure 7E,7F,7G), but we cannot distinguish whether the unlabelled foci are transcriptionally inactive or contain too little Br-RNA to be detected. However, there is no correlation between the amounts of DNA and Br-RNA in a focus (Figure 7K), which is consistent with some being inactive.

Mitochondrial transcription sites lie near extra-mitochondrial ribosomes

We might expect mitochondrial ribosomes to translate co-transcriptionally like their relatives – the bacterial ribosomes – and because the amino-terminal domain of the mitochondrial RNA (mtRNA) polymerase can interact with the mitochondrial translation machinery [41]. Therefore, we wished to label mitochondrial translation sites. Unfortunately, appropriate antibodies to mitochondrial ribosomes are not available, and the labelled precursors (that is, biotin-lys-tRNA, BODIPY-lys-tRNA) that we use to mark extra-mitochondrial translation sites with high resolution [42] cannot be used here; mitochondria contain high concentrations of biotinylated proteins that provide a high background [43] and BODIPY has a similar emission spectrum to YFP. However, proteins encoded by the mitochondrial genome do complex with others encoded by the nuclear genome to form the mitochondrion, and we reasoned that the different synthetic machineries might lie close together on different sides of the mitochondrial membranes so the proteins they produce could combine together efficiently. Therefore, we localized newly-made mtRNA relative to extra-mitochondrial ribosomes. Cells were grown briefly in BrU, fixed, and the resulting mitochondrial Br-RNA localized relative to S6, an extra-mitochondrial ribosomal protein. Most S6 is found in discrete foci remote from mitochondria; these presumably contain clusters of cytoplasmic ribosomes. However, some foci lie close to mitochondrial foci containing Br-RNA (Figure 8A,8B,8C), and this close association was confirmed by cross-correlation analysis (Figure 8D). Newly-made mtRNA also lies near foci containing nascent peptide associated protein (NAC) (Figure 8E,8F,8G,8H), a complex involved in directing nascent cytoplasmic polypeptides to the appropriate cellular compartment and which is known to associate with mitochondrial membranes [44]. Newly-made mtRNA also colocalizes with Tom 22 (Figure 8I,8J,8K,8L), a component of the machinery that imports nuclear-encoded proteins into mitochondria [11,12]. These results are consistent with an association of the mitochondrial transcription and translation machinery on one side of the mitochondrial membrane with the cytoplasmic translation machinery and import machinery on the other.

Discussion

Organization and dynamics of mtDNA

We analyzed the organization and function of mitochondrial DNA (mtDNA) in a stable cell line containing mitochondria tagged with the yellow fluorescent protein (YFP). A plasmid encoding subunit VIII of cytochrome c oxidase fused with YFP, was transfected into ECV304 cells – an epithelial-like human line – and a clone (that is, cox18) expressing YFP established. The tagged subunit is incorporated into mitochondria, so that they autofluoresce (Figure 1A).

As others have found [18,19], mtDNA is concentrated in discrete foci in both fixed and living cells (Figures 1, 2, 4). We calculated the average number of mitochondrial genomes in a focus after measuring the genome number per cell, the total mitochondrial length, and the number of foci per unit length of the mitochondrion (Table 1). While the first two can be measured reasonably accurately, it is difficult to be sure that we detect most foci. Therefore we used various approaches, reasoning that if different methods with different thresholds of detection gave similar results, one estimate would lend credibility to another. Four independent methods (involving immunolabelling with two different antibodies, analysis of profiles of the amount of DNA per focus, packing densities, and replication time) suggest that each focus contains 6–10 genomes (Table 1, line 6), which is again consistent with earlier results [19].

The mtDNA foci are attached to the cytoskeleton as they remain after most soluble proteins are extracted (Figure 2B) [22-24]. Three regions roughly equally spaced around the genome – the origin of replication of the heavy strand plus the heavy- and light-strand promoters, the light strand origin, and another region – are likely candidates for the DNA sequences responsible for attachment, as these sequences remain attached after exhaustive nucleolytic detachment [23]. Then we can imagine the mtDNA is

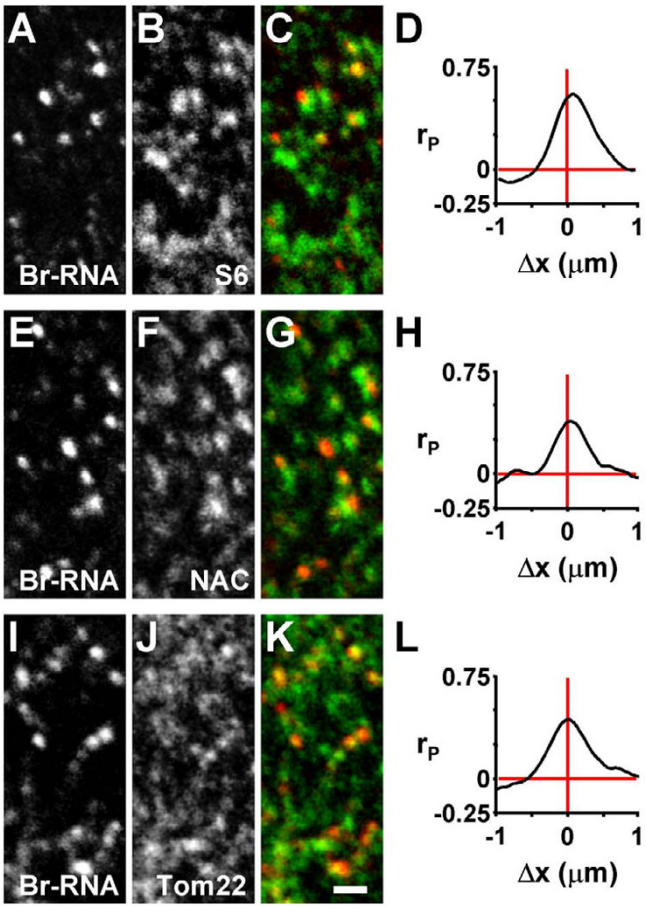

Figure 8
Localization of the cytoplasmic translation and mitochondrial import machinery relative to newly-made mitochondrial transcripts. Cells were grown in BrU for 30 min, fixed, Br-RNA plus different targets immunolabelled, and confocal images collected. Under the conditions used, little Br-RNA made in the nucleus has time to reach the cytoplasm [39]. **(A-C)** Three views of one field; newly-made mitochondrial Br-RNA is found near S6, a constituent of the cytoplasmic ribosome (shown as red and green in the merge in (C), respectively). **(D)** The high Pearson's coefficient (r_P) at Δx values close to zero confirms that Br-RNA is often found near S6. **(E-L)** As (A-D); newly-made mitochondrial Br-RNA is also found near the α subunit of NAC (a cytoplasmic chaperone), and Tom22 (a component of the mitochondrial import machinery). Bar: 1 μm.

tethered (directly or indirectly) through the mitochondrial membranes to the kinesin motor implicated in moving mitochondria along microtubules, as a component of that motor – KIF5B [25] – often colocalizes with foci (Figure 3E,3F,3G,3H). Such a transmembrane linkage implies a specialized structure. This may be related to the transmembrane structures seen in trypanosomes connecting mitochondrial nucleoids to the cytoskeleton [45], and in yeast where they seem to play a role in replication [46].

The limited movement of mtDNA in living cells is also consistent with such a tethering. Cells were grown briefly in ethidium, washed, and regrown in its absence; then fluorescent mtDNA foci can be seen moving in a constrained random walk within the (moving) mitochondria [29]. The foci have a low apparent diffusion constant of 1.1×10^{-3} μm²/s (Figure 4), which is comparable to that of the nuclear DNA of flies [30] but 10-fold higher than that of humans [47]. As the foci move, some split, others fuse (Figure 5A,5B), and still others fuse to remain together for several minutes before splitting; in 49 out of 50 of such fusion-fission events the emerging foci retain the intensity of fusing foci implying that their contents do not mix. Whole mitochondria also split after progressive thinning next to mtDNA foci (Figure 5C) [32], and this can generate daughters without any mtDNA, albeit rarely. Fission next to foci was confirmed in fixed cells; the tips of mitochondria contain mtDNA more often than expected by chance (Figure 1A,1B, insets; see Results). Moreover, the dynamin-related cytoplasmic protein Drp1 is found at fission sites [34], and it often lay immediately next to mtDNA foci (Figure 5D,5E,5F). These results confirm and extend those of Garrido *et al.* [35].

Replication

While nuclear DNA is replicated only during S phase, mtDNA molecules can be replicated at any stage in the cell cycle [32]. Some of the models that can be envisaged for the replication of molecules within a focus are illustrated in Figure 6E. For example, a focus might constitute a unit of replication in which all genomes in that focus initiate coordinately (model a). Alternatively, genomes in one focus might replicate successively, before replication switched to another focus (model c). At the other extreme, all genomes might replicate independently of all others (model b). The labelling kinetics during growth in BrdU are consistent with the stochastic model b; thus, the number of foci containing Br-DNA increases for 3 h and then remains constant (Figure 6C), and the average intensity per focus initially remains constant for 2 h before increasing (Figure 6D). Inevitably, then, some molecules will be re-replicated during one cell cycle, as has been shown previously [32].

Transcription

Sites containing newly-made nuclear RNA can be visualized after growing cells in bromouridine (BrU), and then immunolabelling the resulting Br-RNA [38,39]. We show here the same approach can be used to mark newly-made mitochondrial RNA; moreover, the resulting Br-RNA accumulates in discrete foci (Figure 7A,7B,7C,7D) that

initially colocalize with mtDNA foci (Figure 7E,7F,7G). Pulse-chase experiments reveal this newly-made Br-RNA has a half-life of ~45 min (Figure 7I), and a residence half-time in the mtDNA foci of ~43 min (Figure 7J). This residence half-time is approximately eight-fold longer than the ~5.5 min required to make a complete transcript (calculated assuming ~50 nucleotides are polymerized every second) [40]. This suggests that newly-made mitochondrial messages remain at transcription sites for extended periods, before they are degraded at those sites.

Translation

Mitochondria are formed by proteins encoded by both mitochondrial and nuclear genomes. We reasoned the cytoplasmic machinery generating nuclear-encoded proteins might lie immediately next to its counterpart generating mitochondrial-encoded proteins so both sets of products could combine together efficiently. Therefore, we localized newly-made mtRNA relative to two components of the extra-mitochondrial translation machinery – a ribosomal protein (S6) and a chaperone (NAC) responsible for directing nascent cytoplasmic polypeptides to mitochondria [44] – and to a component of the machinery (Tom22) that imports nuclear-encoded proteins into mitochondria [11,12]; it localized with all three (Figure 8).

Conclusions

The position of mitochondria within the cell is determined largely by the cytoskeleton. For example, the yeast nucleoid is anchored to the cytoskeleton through the inner mitochondrial membrane via Mgm1p (in the intermembrane space) and Mmm1p (in the outer membrane) [2,7,8,48,49]; this anchorage provides a mechanism whereby mtDNA might be replicated, segregated, and inherited [46]. Our results suggest that many of the clusters of 6–10 mitochondrial genomes in a human cell have an even more extensive sphere of influence that includes the translation machineries on both sides of the mitochondrial membranes (Figure 9). Then, proteins encoded by the nuclear genome and destined for the mitochondria will be made close to mitochondrial-encoded proteins so that they can be assembled efficiently into mitochondrial complexes. Moreover, depleting mitochondrial DNA should directly affect mitochondrial structure, which it does [50]. According to this view, mtDNA acts as a central hub that organizes its immediate surroundings both within – and outside – the mitochondrion; one result would be an integration of mitochondrial and cellular protein synthesis.

Methods

Cells

Plasmid pEYFP-Mito encoding subunit VIII of cytochrome c oxidase tagged with YFP (BD Clontech UK, Basingstoke,

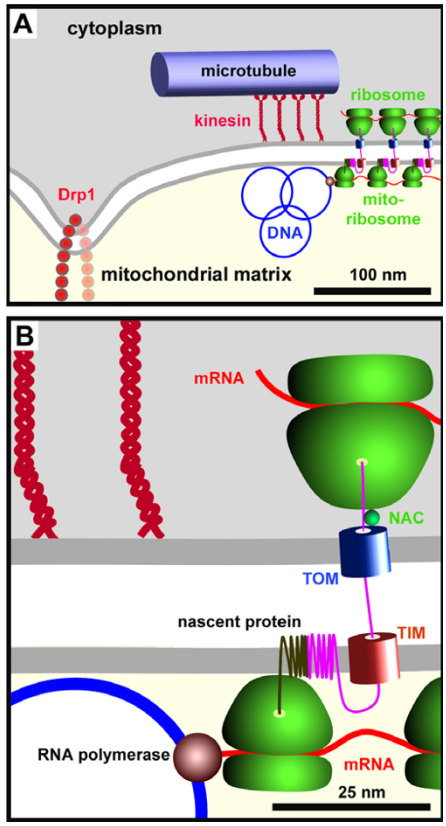

Figure 9

A cartoon illustrating the components studied here (drawn roughly to scale) that lie within the sphere of influence of mtDNA. **(A)** A cluster of approximately eight mitochondrial genomes (see Table 1; only three are shown) are tethered through the mitochondrial membranes (see Figure 2) to kinesin and cytoplasmic microtubular network (see Figure 3); tethering restricts motion (see Figure 4), but the molecular mechanism is unknown. A cluster is usually found in a thin part of the mitochondrion poor in YFP-cytochrome oxidase (Figure 1G), and mitochondria generally split near Drp1 foci lying ~300 nm away (Figure 5). **(B)** A high-power view of a region in (A). Nascent mtRNA is translated cotranscriptionally by mitochondrial ribosomes bound both to the polymerase [40] and the inner mitochondrial membrane [57]; completed mRNAs (not shown) are also translated during most of their lifetime in this region (Figure 7J). The cytoplasmic translation machinery that makes nuclear-encoded proteins destined for the mitochondrion – marked by a ribosomal protein (S6) and a chaperone (NAC) – lie immediately on the other side of the mitochondrial membrane (Figure 8A,8B,8C,8D,8E,8F,8G,8H). Here, a cytoplasmic peptide is being made and imported through the translocases in the outer and inner membranes (TOM and TIM; TOM is marked by Tom22; Figure 8I,8J,8K,8L) where it will assemble with a mitochondrial-encoded peptide in the inner mitochondrial membrane. The close proximity of the two sets of machinery on each side of the membranes ensures efficient assembly of mitochondrial complexes containing proteins encoded by nuclear and mitochondrial genomes.

Hampshire, UK) was transfected into ECV304 (T-24) cells – an epithelial-like human female line derived from a urinary bladder carcinoma [16] – and a stable line with fluorescent mitochondria selected. This clone (cox18) was grown in DMEM supplemented with 10% FCS. For Figures 1C,1D and 6, medium was supplemented with 50 μM bromodeoxyuridine (BrdU; Sigma-Aldrich, Poole, Dorset, UK).

General immunofluorescence

Cells on coverslips were fixed (20 min; 4°C) in 4% paraformaldehyde in 250 mM HEPES (pH 7.4), and antigens indirectly immunolabelled [42] using the following antibodies (unless stated otherwise, Affinipure or multiple labelling grade from Jackson ImmunoResearch, Bar Harbor, ME, USA): (i) monoclonal anti-DNA produced in our laboratory (mouse IgM; 5 μg/ml) + donkey anti-mouse IgM conjugated with Cy3 or Cy5 (0.5 μg/ml); (ii) affinity-purified mouse anti-BrdU (2 μg/ml; Caltag Laboratories, Burlingame, CA, USA) + donkey anti-mouse IgG conjugated with Cy3 (0.5 μg/ml); (iii) anti-tubulin (α-subunit; 1/100; Sigma-Aldrich) + donkey anti-mouse IgG conjugated with Cy3 (0.5 μg/ml); (iv) anti-KIF5B (1/100; PCP42 antibody) [51] + donkey anti-rabbit conjugated with Cy3 (0.5 μg/ml); (v) anti-Drp1 (1/100) [34] + donkey anti-rabbit IgG conjugated with Cy3 (0.5 μg/ml); (vi) anti-Br-RNA (as for anti-BrdU) + donkey anti-mouse IgG conjugated with Cy3 (0.5 μg/ml), (vii) anti-S6 (2 μg/ml; Cell Signalling, Beverley, MA, USA; this antibody yields one band in immunoblots of whole cell extract, and so we assume it does not cross-react with a subunit of the mitochondrial ribosome) + donkey anti-rabbit IgG conjugated with Cy3 (0.5 μg/ml); (viii) anti-NAC (α subunit; 1/250) [52] + donkey anti-rabbit IgG conjugated with Cy3 (0.5 μg/ml); (ix) anti-Tom22 C-terminus (1/500) [53] + donkey anti-rabbit IgG conjugated with Cy3 (0.5 μg/ml). Coverslips were mounted in Vectashield (Vector Laboratories Inc., Burlingame, CA, USA), and images generally collected at 20°C using Lasersharp software and a Nikon TE300 (objective: 60×, numerical aperature 1.4) attached to a BioRad Radiance 2000 confocal microscope (BioRad Laboratories, Hemel Hampstead, UK) [42]. Images were analyzed using EasiVision (Soft Imaging Systems GmbH, Münster, Germany) and Excel (Microsoft) software; single confocal images were also exported from Lasersharp into Photoshop (Adobe Systems Inc., San Jose, California, USA), contrast stretched, and presented without further modification. In Figure 1E, integrated intensities in areas of ≥4 pixels were measured using EasiVision. In Figs 1E and 7J, random distributions were generated (>1,000 runs) using Excel, and $P(l) = e^{-\rho l}$, where $P(l)$ is the probability, ρ is density of foci/μm (Table 1), and l is length in μm.

Immunolabelling Br-DNA

After incubation in BrdU and fixation (above), cells were treated (10 min) in 1% Triton X100 in PBS, rinsed in PBS, and DNA denatured (20 min) with 0.5 M HCl; cells were then washed thoroughly in PBS and immunolabelled with the anti-BrdU (above).

Colocalization analysis

Two-colour images were collected using the confocal microscope (10× zoom; 40 nm pixel size), a line profile of intensities in both channels along mitochondria collected using EasiVision, and data exported to Excel. Pixel intensities in each channel were shifted manually pixel by pixel, and Pearson's coefficient computed [20].

Number of mitochondrial genomes per cell

A total of 10^6 cells were resuspended in 100 μl agarose (1% final concentration in PBS); after gelling, the block was treated successively with 0.5% SDS (30 min), 10 mg/ml RNase A in 10 mM Tris, 1 mM EDTA (1 h), and 100 μg/ml proteinase K (1 h). Blocks and known weights of plasmid DNA were applied to an agarose gel, the gel run (4 h) to resolve mtDNA, and – after staining with ethidium and illumination with uv light – the amount of mtDNA was determined by comparing intensities with those given by plasmid DNA.

Immuno-electron microscopy

For Figure 2A, cells were fixed, treated with osmium, embedded in Epon, indirectly immunolabelled on ultrathin sections, contrasted with uranyl acetate, and digital images collected on a Zeiss 912 Omega electron microscope [39]. DNA was detected using anti-DNA (above) + goat anti-mouse IgM conjugated with 10 nm particles (1:25 dilution; British BioCell International through Agar Scientific, Stanstead, Essex, UK). The diameters of clusters of gold particles seen in images were corrected for the effects of sectioning [54] as follows. The major (2x) and minor (2y) orthogonal axes of each cluster were measured, and the cluster diameter, D calculated from $D = 2\sqrt{(xy)}$. The mean cluster diameter, $\overline{D}$, was calculated from the number of clusters (N) and the diameter of individual clusters (D_1, D_2,...D_N) using

$$\overline{D} = \frac{\pi}{2}\left(\frac{N}{\frac{1}{D_1} + \frac{1}{D_2} + \cdots \frac{1}{D_N}}\right)$$

For Figure 2B, cells were grown (24 h) on 200 mesh nickel grids covered with a formvar film (Agar Scientific), treated (5 min; 4°C) with 0.05% Triton X-100 in cytoskeleton (CSK) buffer [55], washed three times with CSK buffer, fixed (30 min) with 4% paraformaldehyde in CSK buffer, and DNA indirectly immunolabelled using anti-DNA +

goat anti-mouse IgM conjugated with 10 nm particles (as above); finally, grids were dried past the critical point and digital images collected on the Zeiss 912 [39].

Time-lapse movies of mtDNA in living cells

Cells were grown (30 min) in 0.1 μg/ml ethidium, washed with media, regrown in its absence in a heated chamber on the confocal microscope at 37°C, and images collected every 10 seconds using a large confocal pinhole of 5 mm to optimize survival rather than resolution. Coordinates of the gravity center of each ethidium (mtDNA) focus were obtained using EasiVision; data were exported to Excel for analysis, and the mean square displacement (MSD) and autocorrelation coefficient derived [30]. As mtDNA foci move only in one dimension, the diffusion constant was calculated using $12D\Delta t = <\Delta d^2>$, where D is the apparent diffusion coefficient and Δd is the changes in distance seen between foci at increasing time intervals (Δt). RNA was detected in permeabilized and fixed cells using RNase A tagged with Cy3 (prepared using a kit from Molecular Probes Inc., Leiden, The Netherlands) instead of the analogous enzyme:gold complex [56].

Visualizing newly-made transcripts

Cells on coverslips were grown [39] in 2.5 mM bromouridine (BrU; Sigma-Aldrich), fixed (20 min; 4°C) in 4% paraformaldehyde in 250 mM HEPES (pH 7.4), and Br-RNA indirectly immunolabelled using mouse anti-BrdU (Caltag) and donkey anti-mouse Fc conjugated with Cy3. For pulse-chase experiments, cells were grown in BrU, washed in medium without BrU, and regrown in medium with 5 mM U. DNA was labelled using anti-DNA plus donkey anti-IgM conjugated with Cy5 (as above) or with Hoechst 33342 (100 ng/ml; 30 min). Images were collected using a Zeiss Axioplan 2 fluorescence microscope fitted with a SPOT2 CCD camera (Optivision Yorkshire Ltd, West Yorkshire, UK). The distance between foci was calculated in images like Figure 7B,7D as follows. The area, intensity, and position (that is, gravity center) of each focus was determined using EasiVision and the distance to the nearest mtDNA foci calculated using Excel. The random distribution for Figure 7J was generated as above. The residence half-life of Br-RNA in the mtDNA foci was calculated using Berkeley Madonna software (Berkeley, CA, USA). We assume the cellular concentration of BrU (and nucleotide triphosphates (NTPs)) remains constant as the BrU is incorporated continuously into Br-RNA that colocalized with mtDNA foci, before the Br-RNA disappears exponentially from those foci during the chase either through export and/or degradation. Then, $d/dt[\text{Br-RNA}] = k_1[\text{NTP}] - k_2[\text{Br-RNA}]$, and the half-life is estimated from k_2.

Abbreviations

ac, autocorrelation coefficient; au, arbitrary units; Br-DNA, DNA containing bromodeoxyuridine; Br-RNA, RNA containing bromouridine; BrdU, bromodeoxyuridine; BrU, bromouridine; CSK buffer, cytoskeleton buffer; DAPI, 4',6'-diamidino-2-phenylindole; MELAS, mitochondrial encephalopathy with lactic acidosis and stroke-like episodes; mtDNA, mitochondrial DNA; mtRNA, mitochondrial RNA; MERFF, myoclonic epilepsy with ragged red fibres; MSD, mean square displacement; NAC, nascent peptide associated protein; NTPs, nucleotide triphosphates; r_P, Pearson's correlation coefficient; YFP, yellow fluorescent protein.

Authors' contributions

FJI and HK conceived of the study, and PRC participated in its design and coordination. HK and FJI generated the cell line, FJI carried out all other experiments and performed the mathematical analyses, and FJI and PRC wrote the manuscript. All authors read and approved the final manuscript.

Acknowledgements

We thank A.M. van der Bliek, E. Jones, M. Mori, R. St. Arnaud, and R. Vale for antibodies against Drp1, DNA, Tom22, NAC, and KIF5B respectively, D. Mason and J. Vazquez for help with analyzing data, and the Spanish Ministerio de Educación y Cultura and the Wellcome Trust for support.

References

1. Hermann GJ, Shaw JM: **Mitochondrial dynamics in yeast.** *Annu Rev Cell Dev Biol* 1998, **14:**265-303.
2. Yaffe MP: **The machinery of mitochondrial inheritance and behavior.** *Science* 1999, **283:**1493-1497.
3. Otsuga D, Keegan BR, Brisch E, Thatcher JW, Hermann GJ, Bleazard W, Shaw JM: **The dynamin-related GTPase, Dnm1p, controls mitochondrial morphology in yeast.** *J Cell Biol* 1998, **143:**333-349.
4. Labrousse AM, Zappaterra MD, Rube DA, van der Bliek AM: ***C. elegans* dynamin-related protein DRP-1 controls severing of the mitochondrial outer membrane.** *Mol Cell* 1999, **4:**815-826.
5. Santel A, Fuller MT: **Control of mitochondrial morphology by a human mitofusin.** *J Cell Sci* 2001, **114:**867-874.
6. Knowles MK, Guenza MG, Capaldi RA, Marcus AH: **Cytoskeletal-assisted dynamics of the mitochondrial reticulum in living cells.** *Proc Natl Acad Sci USA* 2002, **99:**14772-14777.
7. Yaffe MP: **Dynamic mitochondria.** *Nat Cell Biol* 1999, **1:**E149-150.
8. Karbowski M, Spodnik JH, Teranishi M, Wozniak M, Nishizawa Y, Usukura J, Wakabayashi T: **Opposite effects of microtubule-stabilizing and microtubule-destabilizing drugs on biogenesis of mitochondria in mammalian cells.** *J Cell Sci* 2001, **114:**281-291.
9. Shadel GS, Clayton DA: **Mitochondrial DNA maintenance in vertebrates.** *Annu Rev Biochem* 1997, **66:**409-435.
10. Shoubridge EA: **The ABCs of mitochondrial transcription.** *Nat Genet* 2002, **31:**227-228.
11. Hoogenraad NJ, Ward LA, Ryan MT: **Import and assembly of proteins into mitochondria of mammalian cells.** *Biochim Biophys Acta* 2002, **1592:**97-105.
12. Truscott KN, Brandner K, Pfanner N: **Mechanisms of protein import into mitochondria.** *Curr Biol* 2003, **13:**R326-R337.
13. Smeitink J, van den Heuvel L, DiMauro S: **The genetics and pathology of oxidative phosphorylation.** *Nat Rev Genet* 2001, **2:**342-352.
14. Jacobs HT, Lehtinen SK, Spelbrink JN: **No sex please, we're mitochondria: a hypothesis on the somatic unit of inheritance of mammalian mtDNA.** *Bioessays* 2000, **22:**564-572.

15. Birky CW: **The inheritance of genes in mitochondria and chloroplasts: laws, mechanisms, and models.** *Annu Rev Genet* 2001, **35:**125-148.
16. Schneider MU, Troye M, Paulie S, Perlmann P: **Membrane-associated antigens on tumor cells from transitional-cell carcinoma of the human urinary bladder. I. Immunological characterization by xenogeneic antisera.** *Int J Cancer* 1980, **26:**185-192.
17. Partikian A, Olveczky B, Swaminathan R, Li Y, Verkman AS: **Rapid diffusion of green fluorescent protein in the mitochondrial matrix.** *J Cell Biol* 1998, **140:**821-829.
18. Miyakawa I, Sando N, Kawano S, Nakamura S, Kuroiwa T: **Isolation of morphologically intact mitochondrial nucleoids from the yeast, *Saccharomyces cerevisiae*.** *J Cell Sci* 1987, **88:**431-439.
19. Satoh M, Kuroiwa T: **Organization of multiple nucleoids and DNA molecules in mitochondria of a human cell.** *Exp Cell Res* 1991, **196:**137-140.
20. van Steensel B, van Binnendijk EP, Hornsby CD, van der Voort HT, Krozowski ZS, de Kloet ER, van Driel R: **Partial colocalization of glucocorticoid and mineralocorticoid receptors in discrete compartments in nuclei of rat hippocampus neurons.** *J Cell Sci* 1996, **109:**787-792.
21. Collins TJ, Berridge MJ, Lipp P, Bootman MD: **Mitochondria are morphologically and functionally heterogeneous within cells.** *EMBO J* 2002, **21:**1616-1627.
22. Albring M, Griffith J, Attardi G: **Association of a protein structure of probable membrane derivation with HeLa cell mitochondrial DNA near its origin of replication.** *Proc Natl Acad Sci USA* 1977, **74:**1348-1352.
23. Jackson DA, Bartlett J, Cook PR: **Sequences attaching loops of nuclear and mitochondrial DNA to underlying structures in human cells: the role of transcription units.** *Nucleic Acids Res* 1996, **24:**1212-1219.
24. Tolstonog GV, Mothes E, Shoeman RL, Traub P: **Isolation of SDS-stable complexes of the intermediate filament protein vimentin with repetitive, mobile, nuclear matrix attachment region, and mitochondrial DNA sequence elements from cultured mouse and human fibroblasts.** *DNA Cell Biol* 2001, **20:**531-554.
25. Tanaka Y, Kanai Y, Okada Y, Nonaka S, Takeda S, Harada A, Hirokawa N: **Targeted disruption of mouse conventional kinesin heavy chain, kif5B, results in abnormal perinuclear clustering of mitochondria.** *Cell* 1998, **93:**1147-1158.
26. Kellenberger E: **Intracellular organization of the bacterial genome.** In *The bacterial chromosome* Edited by: Drlica K, Riley M. Washington: American Society for Microbiology; 1990:173-186.
27. Dellinger M, Geze M: **Detection of mitochondrial DNA in living animal cells with fluorescence microscopy.** *J Microsc* 2001, **204:**196-202.
28. van Zandvoort MA, de Grauw CJ, Gerritsen HC, Broers JL, oude Egbrink MG, Ramaekers FC, Slaaf DW: **Discrimination of DNA and RNA in cells by a vital fluorescent probe: lifetime imaging of SYTO13 in healthy and apoptotic cells.** *Cytometry* 2002, **47:**226-235.
29. Spelbrink JN, Li FY, Tiranti V, Nikali K, Yuan QP, Tariq M, Wanrooij S, Garrido N, Comi G, Morandi L, Santoro L, Toscano A, Fabrizi GM, Somer H, Croxen R, Beeson D, Poulton J, Suomalainen A, Jacobs HT, Zeviani M, Larsson C: **Human mitochondrial DNA deletions associated with mutations in the gene encoding Twinkle, a phage T7 gene 4-like protein localized in mitochondria.** *Nat Genet* 2001, **28:**223-231.
30. Vazquez J, Belmont AS, Sedat JW: **Multiple regimes of constrained chromosome motion are regulated in the interphase Drosophila nucleus.** *Curr Biol* 2001, **11:**1227-1239.
31. Diggle PJ: *Time series: a biostatistical introduction* New York: Oxford University Press; 1990.
32. Bogenhagen D, Clayton DA: **Mouse L cell mitochondrial DNA molecules are selected randomly for replication throughout the cell cycle.** *Cell* 1977, **11:**719-727.
33. Nunnari J, Marshall WF, Straight A, Murray A, Sedat JW, Walter P: **Mitochondrial transmission during mating in *Saccharomyces cerevisiae* is determined by mitochondrial fusion and fission and the intramitochondrial segregation of mitochondrial DNA.** *Mol Biol Cell* 1997, **8:**1233-1242.
34. Smirnova E, Griparic L, Shurland DL, van der Bliek AM: **Dynamin-related protein Drp1 is required for mitochondrial division in mammalian cells.** *Mol Biol Cell* 2001, **12:**2245-2256.
35. Garrido N, Griparic L, Jokitalo E, Wartiovaara J, van Der Bliek AM, Spelbrink JN: **Composition and dynamics of human mitochondrial nucleoids.** *Mol Biol Cell* 2003, **14:**1583-1596.
36. Davis AF, Clayton DA: **In situ localization of mitochondrial DNA replication in intact mammalian cells.** *J Cell Biol* 1996, **135:**883-893.
37. Magnusson J, Orth M, Lestienne P, Taanman JW: **Replication of mitochondrial DNA occurs throughout the mitochondria of cultured human cells.** *Exp Cell Res* 2003, **289:**133-142.
38. Jackson DA, Iborra FJ, Manders EMM, Cook PR: **Numbers and organization of RNA polymerases, nascent transcripts and transcription units in HeLa nuclei.** *Mol Biol Cell* 1998, **9:**1523-1536.
39. Iborra FJ, Jackson DA, Cook PR: **The path of transcripts from extra-nucleolar synthetic sites to nuclear pores: transcripts in transit are concentrated in discrete structures containing SR proteins.** *J Cell Sci* 1998, **111:**2269-2282.
40. Kornberg A, Baker TA: *DNA replication* 2nd edition. New York: WH Freeman and Co; 1992.
41. Rodeheffer MS, Shadel GS: **Multiple interactions involving the amino-terminal domain of yeast mtRNA polymerase determine the efficiency of mitochondrial protein synthesis.** *J Biol Chem* 2003, **278:**18695-18701.
42. Iborra FJ, Jackson DA, Cook PR: **Coupled transcription and translation within nuclei of mammalian cells.** *Science* 2001, **293:**1139-1142.
43. Hollinshead M, Sanderson J, Vaux DJ: **Anti-biotin antibodies offer superior organelle-specific labeling of mitochondria over avidin or streptavidin.** *J Histochem Cytochem* 1997, **45:**1053-1057.
44. George R, Walsh P, Beddoe T, Lithgow T: **The nascent polypeptide-associated complex (NAC) promotes interaction of ribosomes with the mitochondrial surface in vivo.** *FEBS Lett* 2002, **516:**213-216.
45. Ogbadoyi EO, Robinson DR, Gull K: **A high-order trans-membrane structural linkage is responsible for mitochondrial genome positioning and segregation by flagellar Basal bodies in trypanosomes.** *Mol Biol Cell* 2003, **14:**1769-1779.
46. Meeusen S, Nunnari J: **Evidence for a two membrane-spanning autonomous mitochondrial DNA replisome.** *J Cell Biol* 2003, **163:**503-510.
47. Chubb JR, Boyle S, Perry P, Bickmore WA: **Chromatin motion is constrained by association with nuclear compartments in human cells.** *Curr Biol* 2002, **12:**439-445.
48. Wong ED, Wagner JA, Gorsich SW, McCaffery JM, Shaw JM, Nunnari J: **The dynamin-related GTPase, Mgm1p, is an intermembrane space protein required for maintenance of fusion competent mitochondria.** *J Cell Biol* 2000, **151:**341-352.
49. Hobbs AE, Srinivasan M, McCaffery JM, Jensen RE: **Mmm1p, a mitochondrial outer membrane protein, is connected to mitochondrial DNA (mtDNA) nucleoids and required for mtDNA stability.** *J Cell Biol* 2001, **152:**401-410.
50. Gilkerson RW, Margineantu DH, Capaldi RA, Selker JM: **Mitochondrial DNA depletion causes morphological changes in the mitochondrial reticulum of cultured human cells.** *FEBS Lett* 2000, **474:**1-4.
51. Niclas J, Navone F, Hombooher N, Vale RD: **Cloning and localization of a conventional kinesin motor expressed exclusively in neurons.** *Neuron* 1994, **12:**1059-1072.
52. Yotov WV, Moreau A, St Arnaud R: **The alpha chain of the nascent polypeptide-associated complex functions as a transcriptional coactivator.** *Mol Cell Biol* 1998, **18:**1303-1311.
53. Yano M, Hoogenraad N, Terada K, Mori M: **Identification and functional analysis of human Tom22 for protein import into mitochondria.** *Mol Cell Biol* 2000, **20:**7205-7213.
54. Williams M: **Quantitative methods in biology.** In *Practical Methods in Electron Microscopy Volume 6*. Edited by: Glauert AM. Amsterdam: North-Holland; 1977:48-80.
55. Nickerson JA, Krockmalnic G, Wan KM, Penman S: **The nuclear matrix revealed by eluting chromatin from a cross-linked nucleus.** *Proc Natl Acad Sci USA* 1997, **94:**4446-4450.
56. Bendayan M: **Electron microscopical localization of nucleic acids by means of nuclease-gold complexes.** *Histochem J* 1981, **13:**699-710.

57. Liu M, Spremulli L: **Interaction of mammalian mitochondrial ribosomes with the inner membrane.** *J Biol Chem* 2000, **275:**29400-29406.

Publish with **BioMed Central** and every scientist can read your work free of charge

"BioMed Central will be the most significant development for disseminating the results of biomedical research in our lifetime."

Sir Paul Nurse, Cancer Research UK

Your research papers will be:

- available free of charge to the entire biomedical community
- peer reviewed and published immediately upon acceptance
- cited in PubMed and archived on PubMed Central
- yours — you keep the copyright

Submit your manuscript here:
http://www.biomedcentral.com/info/publishing_adv.asp

BioMedcentral